

**First-principles calculations of piezoelectricity and polarization rotation in  $\text{Pb}(\text{Zr}_{0.5}\text{Ti}_{0.5})\text{O}_3$** 

Zhigang Wu and Henry Krakauer

*Department of Physics, College of William and Mary, Williamsburg, Virginia 23187, USA*

(Received 7 February 2003; published 29 July 2003)

First-principles local-density approximation calculations of the piezoelectric response of  $\text{Pb}(\text{Zr}_{0.5}\text{Ti}_{0.5})\text{O}_3$  (PZT 50/50) are presented for tetragonal and monoclinic phases. We use the linearized augmented plane wave with the local orbital extension method and  $[001]1:1$  ordered PZT 50/50 supercells, constrained with  $P4mm$  tetragonal and  $Cm$  monoclinic symmetry. Calculated internal coordinates of monoclinic PZT 50/50 at the experimental  $c/a$  value are in good agreement with measurements of  $\text{Pb}(\text{Zr}_{0.52}\text{Ti}_{0.48})\text{O}_3$ . Bulk spontaneous polarization, Born effective charges  $Z^*$ , and piezoelectric coefficients are computed using the Berry's phase approach. Greatly enhanced piezoelectric coefficients are observed due to polarization rotation as a function of applied strain in the monoclinic phase with fully relaxed internal atomic coordinates. As the polarization rotates within the  $(1\bar{1}0)$  mirror plane between the  $[001]$  and  $[\nu\nu 1]$  (pseudocubic) directions, values as large as  $e_{33} = 12.6 \text{ C/m}^2$ ,  $e_{15} = 10.9 \text{ C/m}^2$ ,  $e_{13} = -33 \text{ C/m}^2$ , and  $e'_{11} = 36 \text{ C/m}^2$  are observed at  $\nu = 1.27$ , where  $e'_{11}$  is defined as  $0.5(e_{11} + e_{12})$ . Such large values are consistent with the measured piezoelectric response in ceramic PZT. This supports the polarization rotation mechanism as the origin of the enhanced electromechanical response.

DOI: 10.1103/PhysRevB.68.014112

PACS number(s): 77.65.-j, 77.84.Dy

**I. INTRODUCTION**

Complex perovskite alloys of  $A(B'B'')\text{O}_3$  and  $A(B'B''B''')\text{O}_3$  have been extensively studied and widely used in industry because of their excellent piezoelectric properties. Examples include  $\text{Pb}(\text{Zr}_{1-x}\text{Ti}_x)\text{O}_3$  (PZT),<sup>1</sup> which is currently used in acoustic sensors and transducers, and  $(1-x)\text{Pb}(\text{Zn}_{1/3}\text{Nb}_{2/3})\text{O}_3-x\text{PbTiO}_3$  (PZN-PT) and  $(1-x)\text{Pb}(\text{Mn}_{1/3}\text{Nb}_{2/3})\text{O}_3-x\text{PbTiO}_3$  (PMN-PT),<sup>2</sup> which show great promise as acoustic sensors and transducers. All these materials exhibit extremely large piezoelectric coefficients and large electromechanical coupling and strain.<sup>2</sup>

Recently, polarization rotation has been proposed as the origin of high piezoelectric response. It was first advanced by Park and Shrout to explain the giant piezoelectric response in single-crystal piezoelectrics PZN-PT and PMN-PT,<sup>2</sup> and theoretically it was emphasized by first-principles calculations in  $\text{BaTiO}_3$  by Fu and Cohen.<sup>3</sup> Fu and Cohen found that large strain response is induced by an external electric field through polarization rotation, while the strain response for the electric field along the spontaneous polarization direction is small.<sup>3</sup> Their strain-vs-field curve is qualitatively similar to what is observed in PZN-8% PT,<sup>2</sup> but the electric field calculated for  $\text{BaTiO}_3$  is much stronger than the measured one for PZN-8% PT. The discovery by Noheda *et al.*<sup>4</sup> of an unexpected monoclinic phase near the morphotropic phase boundary of PZT suggested that the new phase might serve as a bridge between the tetragonal and orthorhombic phases. Subsequent effective Hamiltonian calculations by Bellaiche *et al.*<sup>5</sup> also showed this behavior. Similar polarization rotation has been observed in PZN-8% PT (Ref. 6) via an orthorhombic intermediate phase. The existence of such intermediate phases has been established on general principles by Vanderbilt and Cohen.<sup>7</sup>

Previous first-principles studies have largely calculated only collinear piezoelectric constants, in which the change in

polarization direction is parallel to the initial polarization direction.<sup>8-10</sup> For example, Sághi-Szabó *et al.* calculated  $e_{33}$  ( $P4mm$ ) =  $4.81 \text{ C/m}^2$  and  $e_{33}$  ( $I4mm$ ) =  $3.60 \text{ C/m}^2$  for single-crystal tetragonal  $\text{Pb}(\text{Zr}_{0.5}\text{Ti}_{0.5})\text{O}_3$  (PZT 50/50).<sup>9</sup> Employing the virtual crystal approximation within the density-functional theory, Bellaiche and Vanderbilt<sup>11</sup> obtained  $e_{33} = 4.4 \text{ C/m}^2$  for tetragonal PZT 50/50. However the measured value of poled ceramic PZT 50/50 (Refs. 12 and 13) is more than twice as large as the first-principles results. Calculations of noncollinear piezoelectric coefficients have been based on effective Hamiltonians, which only depend on a few degrees of freedom and which are fitted to results of first-principles calculations. Bellaiche *et al.*<sup>5</sup> reported a large value of  $d_{15}$  in single-crystal PZT based on their effective Hamiltonian calculations. Using an angular average of their calculated  $d_{15}$ ,  $d_{31}$ , and  $d_{33}$  to simulate a ceramic sample, they obtained good agreement with the measured value of  $d_{33}$  in tetragonal ceramic PZT near the morphotropic phase boundary. They also found that applying an electric field along the pseudocubic  $[111]$  direction introduces the expected phase-transition sequence tetragonal-monoclinic-rhombohedral. Their effective Hamiltonian method only included polar degrees of freedom and did not include competing antiferrodistortive instabilities, which are energetically close, as emphasized by Fornari and Singh.<sup>14</sup>

In this paper, we present direct first-principles calculations of the piezoelectric response of a Zr/Ti chemically ordered model of PZT 50/50. Our first-principles approach treats all competing instabilities on an equal footing, but they are performed at zero temperature and neglect  $B$ -site disorder. To our knowledge, these are the first *ab initio* calculations to yield a large piezoelectric response, which is shown to result from the rotation of the polarization in the monoclinic  $Cm$  mirror plane.<sup>15</sup> The size of the piezoelectric coefficients is commensurate with measured values in  $B$ -site disordered ceramic PZT.

## II. THEORETICAL METHOD

The calculations are performed within the framework of the local-density approximation, and we used the first-principles all-electron linearized augmented plane-wave (LAPW) plus local-orbital method.<sup>16</sup> The local-orbital extension yields the most accurate treatment of atoms with extended semicore orbitals, allowing them to be treated variationally along with the valence bands in a single energy window. Local orbitals were associated with the Zr 4s, 4p; Ti 3s, 3p; and O 2s states. Core states were calculated fully relativistically in an atomiclike approximation using the self-consistent crystal potential. The valence states were treated scalar relativistically, and the Wigner exchange-correlation parametrization was used. Muffin-tin radii were set to 1.85, 1.65, 1.65, and 1.55 a.u. for Pb, Zr, Ti, and O, respectively. Because these calculations are so demanding, for computational simplicity a ten-atom [001]1:1 *B*-site ordered supercell was chosen. The volume was kept fixed at the experimental value of low-temperature microcrystalline monoclinic PZT 50/50.<sup>17</sup> The LAPW convergence parameter  $RK_{max}=6.5$  yielded about 1200 LAPW's, which gave adequately converged results. The special  $\mathbf{k}$ -points method<sup>18</sup> was used to sample the Brillouin zone with a  $4 \times 4 \times 4$  mesh. To relax the internal atomic coordinates, atomic forces following the formulation of Yu *et al.*<sup>19</sup> were calculated. A Secant and Polak-Ribière style conjugate gradient method was implemented, and atomic positions were relaxed until all atomic forces were smaller than 1 mRy/bohr (25.7 meV/Å).

The refined experimental structure<sup>20</sup> of  $\text{Pb}(\text{Zr}_{0.52}\text{Ti}_{0.48})\text{O}_3$  (PZT 52/48) (discussed below) corresponds to a five-atom primitive cell with an averaged Zr/Ti *B*-site atom. It is described using a conventional ten-atom *Cm* monoclinic unit cell with a pseudocubic  $(1\bar{1}0)$  mirror plane. The doubled monoclinic cell has lattice parameters  $\mathbf{a}_m$  and  $\mathbf{b}_m$ , which are directed along the pseudocubic  $[110]$  and  $[1\bar{1}0]$  directions, respectively, and  $\mathbf{c}_m$ , which is directed very close to the  $[001]$  direction. The tilt angle of  $\mathbf{c}_m$  away from the  $[001]$  direction is very small (less than  $0.5^\circ$ ), and the difference of magnitudes between  $a_m$  and  $b_m$  is also small ( $\sim 0.2\%$ ). Due to the small value of these deviations, all our calculations set the tilt angle to zero and  $a_m = b_m$ . *Cm* is a subgroup of both tetragonal *P4mm* and rhombohedral *R3m* structures. With *P4mm* symmetry, our ten-atom primitive unit cell of  $[001]1:1$  *B*-site ordered PZT 50/50 has lattice vectors  $\mathbf{R}_1 = a[1,0,0]$ ,  $\mathbf{R}_2 = a[0,1,0]$ , and  $\mathbf{R}_3 = c[0,0,2]$ . This corresponds to a conventional 20-atom monoclinic cell, whose lattice vectors are  $\mathbf{A}_1 = a[1,1,0]$ ,  $\mathbf{A}_2 = a[1,\bar{1},0]$ , and  $\mathbf{A}_3 = c[0,0,2]$ . The *P4mm*  $c/a$  ratio corresponds to  $2\sqrt{2}c_m/(a_m + b_m)$  with respect to the monoclinic axes.

The piezoelectric tensor is most conveniently calculated from finite differences of the bulk polarization due to applied strain in zero electric field. The change in total macroscopic polarization, containing both electronic and rigid-ionic core contributions, is a well-defined bulk property, which can, in principle, be measured in shorted boundary conditions. The electronic part of the polarization was determined using the Berry's phase approach.<sup>8,21,22</sup> The total polarization of a

strained sample  $\mathbf{P}^T$  can be expressed as  $P_i^T = P_i^s + e_{iv}\epsilon_v$ , where  $P_i^s$  is the spontaneous polarization of the unstrained sample,  $\epsilon_v$  is the strain tensor element, and  $e_{iv}$  defines the piezoelectric tensor elements in Voigt notation.<sup>23</sup> The elements of the macroscopic piezoelectric tensor can be further separated into two parts: a clamped-ion or homogeneous strain contribution evaluated at vanishing internal strain,<sup>24</sup> and an internal strain term that is due to the relative displacements of differently charged sublattices:

$$e_{iv} = e_{iv,c} + e_{iv,i}, \quad (1)$$

where

$$e_{iv,c} = \left. \frac{\partial P_i^T}{\partial \epsilon_v} \right|_u \quad (2)$$

and

$$e_{iv,i} = \sum_k \left. \frac{\partial P_i^T}{\partial u_{k,i}} \right|_\epsilon \frac{\partial u_{k,i}}{\partial \epsilon_v} = \sum_k \frac{ea_i}{\Omega} Z_{k,ii}^* \frac{\partial u_{k,i}}{\partial \epsilon_v}, \quad (3)$$

where  $\Omega$  is the volume,  $a_i$  is the lattice parameter,  $k$  is an atomic index, and  $Z^*$  is the transverse (Born) effective charge:

$$Z_{k,iv}^* = Z_k^{core} + Z_{k,iv}^{*,el} = \left. \frac{\Omega}{ea_i} \frac{\partial P_i^T}{\partial u_{k,v}} \right|_\epsilon. \quad (4)$$

In a ferroelectric material, only changes of the *proper* macroscopic polarization can be measured experimentally:<sup>23,25</sup>  $P_i^P = P_i^T - \sum_j (\epsilon_{ij} P_j^s - \epsilon_{jj} P_i^s)$ . The difference between the proper and total polarizations is due only to the homogeneous part.

Tetragonal *P4mm* PZT has three independent piezoelectric tensor components:  $e_{31} = e_{32}$ ,  $e_{33}$ , and  $e_{15}$ , where  $e_{31}$  and  $e_{33}$  describe the polarization induced along the  $z$  axis when the crystal is uniformly strained in the basal  $xy$  plane or along the  $z$  axis, respectively, and  $e_{15}$  measures the change of polarization perpendicular to the  $z$  axis induced by shear strain. Monoclinic *Cm* PZT has ten independent piezoelectric tensor components,<sup>26</sup> seven of which were calculated:  $e_{33}$ ,  $e_{31}$ ,  $e_{32}$ ,  $e_{13}$ ,  $e_{11}$ ,  $e_{12}$ , and  $e_{15}$ . Here we adopt the convention that the first subscript ( $i=1, 2,$  and  $3$ ) denotes the directions of the conventional monoclinic unit-cell lattice vectors  $\mathbf{A}_1$ ,  $\mathbf{A}_2$ , and  $\mathbf{A}_3$ , respectively. Thus,  $e_{13}$  and  $e_{15}$  describe the polarization induced along the pseudo-cubic  $[110]$  direction by a strain along the  $z$  axis and a shear strain, respectively.

There are both direct and indirect methods to determine piezoelectric tensor elements.<sup>8</sup> In the direct approach the polarization difference is computed as a function of strain, with the internal coordinates optimized at each strain. The slope of  $\Delta P$  vs strain is the piezoelectric constant. In the indirect approach, one can evaluate the clamped-ion term from polarization differences as a function of strain, with the internal parameters kept fixed, and the internal strain term can be calculated from the Born charge tensor and the change of internal coordinates  $u_i$  as a function of strain. Both the direct and indirect methods were used and there is no significant

difference, as expected for small applied strains (typically less than  $\pm 1\%$ ). For the  $\mathbf{k}$ -space integrations in the Berry's phase calculations, a uniform  $4 \times 4 \times 12$   $\mathbf{k}$ -point mesh was found to be adequate.

### III. RESULTS AND DISCUSSION

The morphotropic phase boundary in  $\text{PbZr}_x\text{Ti}_{1-x}$  lies near  $x=1/2$ . According to a recent structural refinement by Noheda *et al.*<sup>20</sup>  $\text{PbZr}_{0.52}\text{Ti}_{0.48}$  at 20 K is in the  $Cm$  monoclinic phase. Section III A compares the calculated atomic positions with the measured values. We next examine trends in the piezoelectric coefficients, first presenting results for the high-symmetry tetragonal  $P4mm$  structure in Sec. III B. Using the  $P4mm$  structure as a reference state, the polarization as a function of  $c/a$  strain is then calculated in Sec. III C to provide an overview of the polarization rotation and piezoelectric response as the structure switches from  $P4mm$  symmetry to  $Cm$  symmetry with decreasing  $c/a$ . For comparison, similar results are presented for  $\text{PbTiO}_3$ . Section III D presents calculated piezoelectric coefficients in the  $Cm$  monoclinic phase. Section III E presents calculations for a related  $P2mm$  orthorhombic structure, whose polarization is rotated by  $90^\circ$  compared to the  $P4mm$  structure.

#### A. Internal coordinates of monoclinic PZT compared with experiment

The structural refinement of  $Cm$  ceramic  $\text{PbZr}_{0.52}\text{Ti}_{0.48}$  at 20 K by Noheda *et al.*<sup>20</sup> is compared to fully relaxed calculations in Table I. The upper part of Table I contains the relaxed theoretical internal coordinates of the ten-atom cell of monoclinic PZT 50/50 at the experimental volume and  $c/a=1.035$ .<sup>20</sup> For comparison, we also present the relaxed internal coordinates of  $P4mm$  tetragonal PZT 50/50 at  $c/a=1.045$  (the minimum-energy  $P4mm$  structure), shown in the upper right of Table I in parentheses. To facilitate comparison with experiment, the bottom panel shows the calculated averaged internal coordinates of every atom in terms of the conventional monoclinic basis vectors. The coordinates are expressed with respect to the Pb atoms in each of the two five-atom perovskite units and their average is given in the bottom panel and compared to the experimental values. Given the neglect of  $B$ -site disorder in the calculation and the slightly different chemical composition, our results are in reasonable agreement with the measured values.

#### B. Piezoelectric coefficients of tetragonal $P4mm$ PZT

Imposing  $P4mm$  symmetry on the ten-atom unit cell and fully relaxing the internal coordinates, the total energy was calculated as a function of  $c/a$  with the volume fixed at the experimental value. The energy is minimized at  $c/a=1.045$ , which is in reasonable agreement with the experimental value of  $c/a=1.029$  for PZT 50/50 at room temperature.<sup>17</sup> The relaxed  $c/a=1.045$  configuration was chosen as the reference state for further polarization calculations. The calculated spontaneous polarization in this state is  $0.81 \text{ C/m}^2$ , which is consistent with  $0.74 \text{ C/m}^2$  obtained by Sági-Szabó *et al.*<sup>9</sup> at the experimental value of  $c/a$  [using a

TABLE I. Internal coordinates of monoclinic  $Cm$  PZT 50/50 ( $c/a=1.035$ ). The upper part of the table gives the relaxed theoretical internal coordinates of the ten-atom cell of monoclinic PZT 50/50 at the experimental volume and  $c/a=1.035$  (Ref. 20). The coordinates ( $u$ ) are given in terms of the lattice constants of the tetragonal ten-atom unit cell, and for comparison, we also present the relaxed internal  $z$  coordinates of  $P4mm$  tetragonal PZT 50/50 at  $c/a=1.045$  in parentheses. The bottom panel gives the calculated averaged internal coordinates in terms of the conventional monoclinic basis vectors (see text), which facilitates comparison with the experimental values given in parentheses.

| Atom               | $x$                         | $y$                         | $z$                           |
|--------------------|-----------------------------|-----------------------------|-------------------------------|
| $u_{\text{Pb}}$    | 0                           | 0                           | 0 (0)                         |
| $u_{\text{Pb}}$    | 0.003                       | 0.003                       | 0.529 (0.531 <sup>a</sup> )   |
| $u_{\text{Zr}}$    | 0.534                       | 0.534                       | 0.245 (0.242 <sup>a</sup> )   |
| $u_{\text{Ti}}$    | 0.520                       | 0.520                       | 0.741 (0.735 <sup>a</sup> )   |
| $u_{\text{O}_1}$   | 0.557                       | 0.040                       | 0.199 (0.186 <sup>a</sup> )   |
| $u_{\text{O}_3}$   | 0.561                       | 0.561                       | 0.487 (0.477 <sup>a</sup> )   |
| $u_{\text{O}_4}$   | 0.553                       | 0.049                       | 0.719 (0.708 <sup>a</sup> )   |
| $u_{\text{O}_6}$   | 0.555                       | 0.555                       | 0.959 (0.949 <sup>a</sup> )   |
| Atom               | $x_m$                       | $y_m$                       | $z_m$                         |
| $u_{\text{Pb}}$    | 0                           | 0                           | 0                             |
| $u_{\text{Zr/Ti}}$ | 0.526 (0.523 <sup>b</sup> ) | 0                           | 0.457 (0.449 <sup>b</sup> )   |
| $u_{\text{O}_1}$   | 0.299 (0.288 <sup>b</sup> ) | 0.255 (0.243 <sup>b</sup> ) | 0.389 (0.373 <sup>b</sup> )   |
| $u_{\text{O}_3}$   | 0.557 (0.552 <sup>b</sup> ) | 0                           | -0.084 (-0.099 <sup>b</sup> ) |

<sup>a</sup>Calculated coordinates for tetragonal  $P4mm$  phase at  $c/a=1.045$ .

<sup>b</sup>Experimental structural refinement from Ref. 20 for monoclinic  $Cm$  ceramic  $\text{PbZr}_{0.52}\text{Ti}_{0.48}$  at 20 K,  $2\sqrt{2}c_m/(a_m+b_m)=1.023$ .

generalized gradient approximation (GGA) for the exchange-correlation potential]. The magnitude of the polarization of the fully relaxed monoclinic structure at  $c/a=1.035$  (coordinates given in Table I) is  $0.80 \text{ C/m}^2$ .

Born effective charges were obtained from finite differences of macroscopic polarization induced by small displacements of atomic sublattices. Our results shown in Table II satisfy the acoustic sum rule,  $\sum_k Z_{k,ii}^* = 0$ , indicating that the calculations are well converged with respect to computational conditions. While many ionic oxides have Born effective charges close to their static values,<sup>27</sup> ferroelectric perovskites display anomalously large dynamical charges<sup>8,9,28,29</sup> similar to those shown in Table II. The Born effective charges have values similar to those in related materials such as  $\text{PbTiO}_3$  (Ref. 8) and PMN-PT.<sup>10</sup>

The calculated piezoelectric tensor elements are listed in Table III. The calculated values of  $e_{33}=4.18 \text{ C/m}^2$  are about half that of values measured in ceramic PZT.<sup>12,13</sup> This is consistent with previous calculations of the collinear piezoelectric effect:  $e_{33}=4.81 \text{ C/m}^2$  by Sági-Szabó *et al.*<sup>9</sup> and  $e_{33}=3.4 \text{ C/m}^2$  by Bellaiche and Vanderbilt<sup>10</sup> Indeed,  $e_{33}$  in PZT is not much larger than the  $3.61\text{-C/m}^2$  value in  $\text{PbTiO}_3$ .<sup>8</sup> The calculated magnitude of  $e_{31}$  is the smallest of those shown in Table III, which is consistent with the experimentally measured values. However, the calculated value is of

TABLE II. Born effective charges for  $P4mm$  symmetry PZT 50/50.  $O_1$  or  $O_4$  is on the  $xz$  face of the unit cell,  $\perp$  marks the direction perpendicular to the Ti-O bond in the  $xy$  plane, and  $\parallel$  indicates atomic displacement along the Ti-O bond.

| Atom  | $Z_{xx}^*$                    | $Z_{yy}^*$                        | $Z_{zz}^*$                |
|-------|-------------------------------|-----------------------------------|---------------------------|
| Pb    | 3.77 (3.74 <sup>a</sup> )     | 3.77                              | 3.46 (3.46 <sup>b</sup> ) |
| Pb    | 3.87                          | 3.87                              | 2.63 (2.83 <sup>b</sup> ) |
| Zr    | 5.56                          | 5.56                              | 5.95 (6.06 <sup>b</sup> ) |
| Ti    | 5.99 (6.20 <sup>a</sup> )     | 5.99                              | 5.27 (5.35 <sup>b</sup> ) |
| $O_1$ | $-2.55_{\perp}$ ( $-2.61^a$ ) | $-4.42_{\parallel}$ ( $-5.18^a$ ) | $-2.33$ ( $-2.33^b$ )     |
| $O_3$ | $-2.34$ ( $-2.15^a$ )         | $-2.34$                           | $-4.65$ ( $-4.79^b$ )     |
| $O_4$ | $-2.85_{\perp}$               | $-4.97_{\parallel}$               | $-1.86$ ( $-1.91^b$ )     |
| $O_6$ | $-2.06$                       | $-2.06$                           | $-4.28$ ( $-4.44^b$ )     |

<sup>a</sup>Reference 8, GGA results for  $PbTiO_3$ .

<sup>b</sup>Reference 9, GGA results at experimental volume and structural parameters.

opposite sign to the measured value. Measured values of piezoelectric coefficients often vary considerably (we are aware of only the measured value in Ref. 12). Even for  $PbTiO_3$ , measured values for  $e_{31}$  range from  $-0.98$  to  $2.1$ . By contrast, the calculated PZT value of  $e_{15} = 10.9$  C/m<sup>2</sup> is more than three times as large as  $e_{15} = 3.15$  C/m<sup>2</sup> in  $PbTiO_3$ .<sup>8</sup> The clamped-ion contributions are similar in PZT and  $PbTiO_3$  ( $e_{15,c}^P = 1.65$  C/m<sup>2</sup> for PZT and  $e_{15,c}^P = 1.99$  C/m<sup>2</sup> for  $PbTiO_3$ ), whereas the internal strain contributions are significantly different ( $e_{15,i} = 9.28$  C/m<sup>2</sup> for PZT and  $e_{15,i} = 1.16$  C/m<sup>2</sup> for  $PbTiO_3$ ). The large value of  $e_{15}$  is actually a manifestation of polarization rotation, since the  $\epsilon_5$  shear strain induces a polarization component perpendicular to the spontaneous polarization directed along the  $z$  direction. In PZT the piezoelectric effect due to polarization rotations is much larger than the collinear response, while in  $PbTiO_3$  the polarization rotation part  $e_{15}$  is similar in size to the collinear  $e_{33}$ . The large calculated value of  $e_{15}$  in PZT is comparable to  $d_{15}$  calculated by Bellaiche and Vanderbilt<sup>11</sup> using the effective Hamiltonian method. We can estimate our corresponding value of  $d_{15}$  using the fact that for  $P4mm$  symmetry  $d_{15} = e_{15}s_{44}$ , where  $s$  is the elastic compliance. Using Berlincourt's value of  $s_{44} = 32.8 \times 10^{-12}$  m<sup>2</sup>/N yields  $d_{15} = 358$  pC/N. This is similar to the large value of  $d_{15} = 550$  pC/N calculated by Bellaiche and Vanderbilt.<sup>11</sup>

TABLE III. Piezoelectric stress tensor elements (C/m<sup>2</sup>) of tetragonal  $P4mm$  PZT 50/50 ( $c/a = 1.045$ , collinear effect of  $e_{33}$ ).

|                         | $e_{33}$                  | $e_{31}$ | $e_{15}$ |
|-------------------------|---------------------------|----------|----------|
| Proper homogeneous      | $-0.68$ ( $-0.65^a$ )     | 1.04     | 1.65     |
| Internal strain         | 4.86 (5.46 <sup>a</sup> ) | 0.92     | 9.28     |
| Proper total            | 4.18 (4.81 <sup>a</sup> ) | 1.96     | 10.9     |
| Experiment <sup>b</sup> | 11.3                      | $-2.67$  | 7.65     |
| Experiment <sup>c</sup> | 11.9                      |          |          |

<sup>a</sup>Reference 9, GGA results at experimental volume and structural parameters.

<sup>b</sup>Reference 12, at room temperature.

<sup>c</sup>Reference 13, at low temperature.

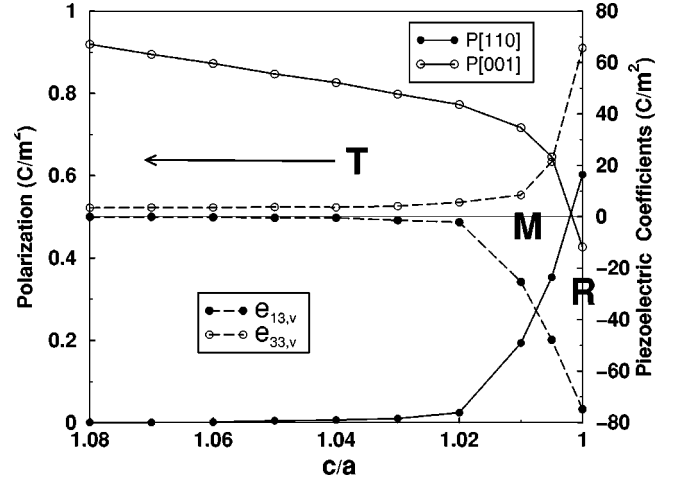


FIG. 1. Piezoelectric response of monoclinic  $Cm$   $PbTiO_3$ . Solid lines denote polarization, and long dashed lines piezoelectric coefficients. Open symbols refer to the [001] direction, and solid symbols to the [110] direction. T, M, and R represent tetragonal, monoclinic, and rhombohedral phases, respectively.

As discussed below, there are lower-symmetry PZT phases that are energetically very close to  $P4mm$  symmetry, unlike the case in  $PbTiO_3$ . This explains the much larger value of  $e_{15}$  in PZT than in  $PbTiO_3$ . This is consistent with the existence in PZT of the observed stable monoclinic phase close to the morphotropic phase boundary, which is where the largest piezoelectric response is obtained.

### C. Polarization rotation in $Cm$ monoclinic $PbTiO_3$ and PZT

The  $c/a$  strain dependence of the polarization in  $Cm$  monoclinic PZT is next studied and compared to that in  $PbTiO_3$ .  $Cm$  symmetry was imposed so the polarization can continuously rotate between the [001] and [111] directions within the  $Cm$  mirror. For  $PbTiO_3$ , the room-temperature experimental volume<sup>30</sup> was used while  $c/a$  was allowed to vary. The Brillouin zone was sampled with a  $4 \times 4 \times 4$  special  $\mathbf{k}$ -point mesh, and the  $\mathbf{k}$ -space integrations in the Berry's phase calculations were made on a uniform  $4 \times 4 \times 20$   $\mathbf{k}$ -point mesh. Fully relaxing the internal coordinates ( $u$ ) at each  $c/a$ ,  $PbTiO_3$  was found to adopt tetragonal symmetry for  $c/a > 1.03$ , as shown in Fig. 1. The lowest-energy  $PbTiO_3$  structure has  $P4mm$  symmetry and  $c/a = 1.07$  ( $c/a = 1.065$  is measured<sup>30</sup>), and its spontaneous polarization is  $0.89$  C/m<sup>2</sup>. The total energy increases as  $c/a$  is reduced from 1.07 to 1.0, i.e., the total energy increases through the sequence of T, M, and R phases. As shown in Fig. 1, the polarization can rotate from [001] to [111] directions in the  $(1\bar{1}0)$  mirror plane. The piezoelectric constants in Fig. 1,  $e_{33,v}$  and  $e_{13,v}$ , are the fixed volume constants  $e_{33}$  and  $e_{13}$ , defined as the following:

$$e_{33,v} \equiv e_{33} - 0.5(e_{31} + e_{32}), \quad e_{13,v} \equiv e_{13} - 0.5(e_{11} + e_{12}). \quad (5)$$

They were calculated from numerical derivatives of the polarization with respect to applied strains. These coefficients become very large in the range  $1.02 < c/a < 1.0$ , where a

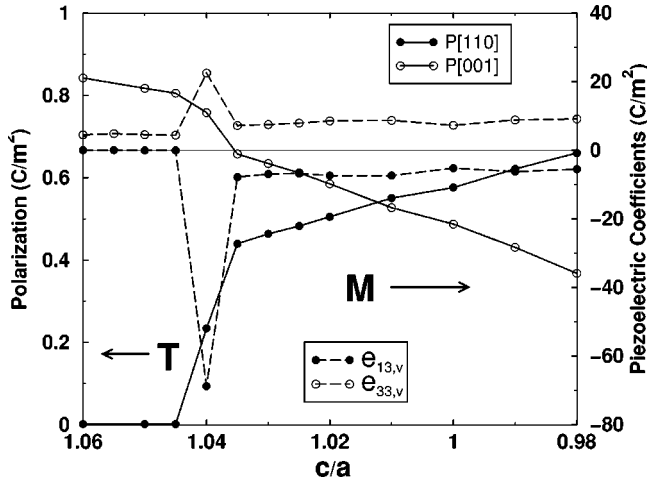


FIG. 2. Piezoelectric response of monoclinic  $Cm$  PZT 50/50. Solid lines denote polarization, and long dashed lines piezoelectric coefficients. Open symbols refer to the [001] direction, and solid symbols refer to the [110] direction. T and M represent tetragonal and monoclinic phases, respectively.

phase transition between monoclinic and rhombohedral symmetry occurs. Peak values in Fig. 1 of  $e_{33,v}$  and  $e_{13,v}$  are as large as  $65 \text{ C/m}^2$  and  $-74 \text{ C/m}^2$ , respectively. However, rhombohedral  $\text{PbTiO}_3$  is  $35 \text{ meV}$  (per five-atom unit) higher in energy than the tetragonal structure. This would require an unrealistically large electric field along the [111] direction to drive  $\text{PbTiO}_3$  from the tetragonal phase to the rhombohedral phase, so these large piezoelectric responses are never seen in pure  $\text{PbTiO}_3$ .

For PZT,  $c/a$  was varied from 0.98 to 1.06 while the volume was fixed at the experimental value. These calculations are very demanding, because the low-symmetry  $Cm$  space group has only two point-group operations. As a result, many more independent  $\mathbf{k}$  points are required during the self-consistent calculations than for  $P4mm$  symmetry. Moreover, the low symmetry leads to 16 independent internal coordinates compared to seven for tetragonal  $P4mm$  PZT. Since the total number of conjugate gradient steps needed to optimize the internal structure is approximately equal to the number of independent internal coordinates, this also adds to the computational burden. The polarization changes smoothly for  $\text{PbTiO}_3$  in Fig. 1, but in Fig. 2, there is an abrupt onset of nonzero  $P[110]$  polarization. Our results show that PZT remains tetragonal for  $c/a \geq 1.045$ , and becomes monoclinic for  $c/a \leq 1.035$ . As shown in Fig. 2, the polarization rotates from pseudocubic [001] to  $[\nu\nu 1]$ , where  $\nu = 1.27$  (corresponding to  $c/a = 0.98$ ), in the  $(1\bar{1}0)$  mirror plane. The polarization changes linearly in the regions of  $c/a \geq 1.045$  and  $c/a \leq 1.035$ , while it changes dramatically in the range of  $1.045 < c/a < 1.035$ , where the values of  $e_{33,v}$  and  $e_{13,v}$  can be as high as  $21 \text{ C/m}^2$  and  $-70 \text{ C/m}^2$ , respectively, as shown in Fig. 2. These large values of piezoelectric constants are consistent with the effective Hamiltonian results.<sup>31</sup> In the effective Hamiltonian calculations,<sup>31</sup> a maximum in some piezoelectric coefficients is observed as the Ti composition decreases in passing from the tetragonal to the rhombohedral phase, via the monoclinic phase. This was also

TABLE IV. Piezoelectric stress tensor elements ( $\text{C/m}^2$ ) of monoclinic  $Cm$  PZT 50/50 ( $c/a = 1.045$ , polarization rotation effect of  $e_{33}$ ).

|                         | $e_{33}$ | $e'_{31}$ | $e_{13}$ | $e'_{11}$ |
|-------------------------|----------|-----------|----------|-----------|
| Proper homogeneous      | -0.68    | 1.04      | 0        | 0         |
| Internal strain         | 13.3     | -8.91     | -33      | 36        |
| Proper total            | 12.6     | -7.87     | -33      | 36        |
| Experiment <sup>a</sup> | 11.3     | -2.67     |          |           |
| Experiment <sup>b</sup> | 11.9     |           |          |           |

<sup>a</sup>Reference 12, at room temperature.

<sup>b</sup>Reference 13, at low temperature.

observed in experiment.<sup>32</sup> Normal values of piezoelectric constants were found in the tetragonal phase for  $c/a \geq 1.045$ , and in the monoclinic phase for  $c/a \leq 1.035$ . The value of  $e_{33,v}$  for the monoclinic phase is nearly twice as large as that for the tetragonal phase.

#### D. Piezoelectric coefficients of monoclinic $Cm$ PZT

In the previous section, an overview of polarization rotation in the  $Cm$  phase was presented, and curves of two constant-volume piezoelectric coefficients were obtained by numerical differentiation of the polarization vs  $c/a$  curve. In this section, we focus on  $c/a = 1.045$ , where the piezoelectric response is large in Fig. 2, and on  $c/a = 1.025$ , the linear region in Fig. 2 where the piezoelectric response is small. At these two  $c/a$  values small finite strains are applied, and several piezoelectric coefficients are obtained from finite differences of the polarization in the usual way (i.e., the volume is not kept constant). Table IV presents the results at  $c/a = 1.045$ . The coefficients  $e'_{31}$  and  $e'_{11}$  in Table IV are defined as

$$e'_{31} \equiv 0.5(e_{31} + e_{32}); \quad e'_{11} \equiv 0.5(e_{11} + e_{12}). \quad (6)$$

$e'_{31}$  can be compared to  $e_{31}$  in Table III, since  $e_{31} = e_{32}$  and  $e_{11} = e_{12}$  in the  $P4mm$  tetragonal structure. The piezoelectric measurements in Table IV were performed prior to the discovery of the monoclinic phase boundary. Moreover, according to the new structural refinement measurements in Ref. 20, low-temperature PZT 48/52 is monoclinic, and at room temperature it is tetragonal. Thus the same measured piezoelectric constants are listed in both Table III and Table IV, since the experimental crystal was nominally tetragonal. Compared with Table III,  $e_{33}$  and  $e'_{31}$  in Table IV are enhanced due to polarization rotation, and very large values of  $e_{13} = -33 \text{ C/m}^2$  and  $e'_{11} = 36 \text{ C/m}^2$  are obtained.

Sághi-Szabó *et al.*<sup>9</sup> derived an experimental value for  $e_{33}$  of ceramic PZT 50/50 from measured room-temperature piezoelectric strain constants  $d_{ij}$  and elastic compliances  $s_{ij}^E$ .<sup>12</sup> Sághi-Szabó *et al.* erroneously obtained the value of  $e_{33} = 27.0 \text{ C/m}^2$ , because they used a positive value of  $d_{31} = 70 \text{ pC/N}$ . Using instead the correct negative value  $d_{31} = -70 \text{ pC/N}$ ,  $e_{33} = 11.3 \text{ C/m}^2$  is obtained. (We note that  $e_{33}$  derived from measurements at room temperature is a little smaller than the  $11.9 \text{ C/m}^2$  derived from measurements at

TABLE V. Piezoelectric stress tensor elements ( $C/m^2$ ) of monoclinic  $Cm$  PZT 50/50 ( $c/a=1.025$ ).

|                    | $e_{33}$ | $e'_{31}$ | $e_{13}$ | $e'_{11}$ | $e_{15}$ |
|--------------------|----------|-----------|----------|-----------|----------|
| Proper homogeneous | -0.55    | 0.78      | 0.63     | -0.16     | 1.57     |
| Internal strain    | 6.70     | -2.11     | -3.43    | 3.56      | 0.08     |
| Proper total       | 6.15     | -1.33     | -2.80    | 3.40      | 1.65     |

low temperature,<sup>13</sup> but this may be due to different sample preparation and experimental conditions.) In Table IV our predicted values for monoclinic PZT are  $e_{33}=12.6 C/m^2$  and  $e'_{31}=-7.87 C/m^2$ . Du *et al.* demonstrated that for tetragonal PZT, the large experimental value of  $d_{33}$  in ceramics is related to their large calculated value of single-crystal  $d_{33}$  using semiempirical simulations.<sup>33</sup> Using the measured  $s_{ij}^E$  and our values in Table IV, we determine  $d_{33}=306 pC/N$ , in good agreement with their value of  $d_{33}=314 pC/N$  for single-crystal tetragonal PZT 50/50. By contrast, we get  $d_{33}=49 pC/N$  using the values in Table III.

We also studied the piezoelectric response in the linear region of the monoclinic phase in Fig. 2. Using the  $c/a=1.025$  structure as the reference state, we obtained the calculated piezoelectric constants listed in Table V. Compared with the tetragonal values in Table III, the homogeneous contributions of  $e_{33}$  and  $e'_{31}$  are slightly smaller, while the internal strain parts are larger. We calculated a negative  $e'_{31}$  for monoclinic PZT. For  $e_{15}$ , the homogeneous part of the monoclinic phase is slightly smaller than that of the tetragonal phase, while the difference in internal strain contributions is large. The small value of  $e_{15,i}=0.08 C/m^2$  may be due to the fact that the shear strain  $\epsilon_5$  is along a direction close to that of spontaneous polarization, resulting in a collinear contribution to  $e_{15}$ . Fu and Cohen calculated a very small piezoelectric response of the rhombohedral phase of BT due to an applied  $\langle 111 \rangle$  electric field.<sup>3</sup> Guo *et al.* reported that the piezoelectric elongation of the rhombohedral PZT is not along  $[111]$ , but along a  $[001]$  direction.<sup>34</sup> Our results are consistent with their calculations and experimental findings.

### E. Quasitetragonal (orthorhombic $P2mm$ ) PZT

We also studied another tetragonal PZT structure, in which the spontaneous polarization is perpendicular to the Zr/Ti chemical ordering direction, so that the spontaneous polarization direction is rotated by  $90^\circ$  with respect to the  $P4mm$  structure. Bellaiche and Vanderbilt<sup>10</sup> have previously calculated  $e_{33}$  in this structure, whose space group is  $P2mm$ . If the chemical ordering is chosen to lie along the  $[100]$  direction, the spontaneous polarization lies along the  $[001]$  direction. The lattice vectors are  $\mathbf{R}_1=a[2,0,0]$ ,  $\mathbf{R}_2=a[0,1,0]$ , and  $\mathbf{R}_3=c[0,0,1]$ . At the experimental volume, our calculations indicate that relaxed  $P2mm$  PZT has  $c/a=1.06$ , larger than Bellaiche and Vanderbilt's  $c/a=1.0345$ , using an ultrasoft pseudopotential method.<sup>10</sup> The optimized volume in Ref. 10 is about 2.6% less than that of experiment, which might explain the discrepancy with our  $c/a$  value obtained at the experimental volume. The spontaneous polar-

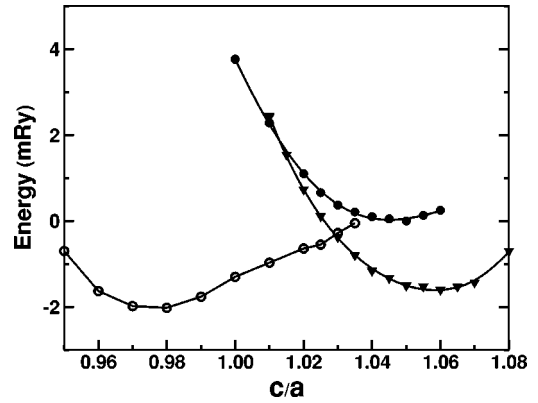


FIG. 3. Total energy (per ten-atom unit cell) of PZT 50/50 as a function of  $c/a$  for some structures. The solid circles, open circles, and solid triangles denote the tetragonal  $P4mm$ , monoclinic  $Cm$ , and “quasitetragonal”  $P2mm$ , respectively.

ization is  $0.84 C/m^2$ , and the calculated piezoelectric constant  $e_{33}=3.50 C/m^2$  is very close to Bellaiche and Vanderbilt's  $e_{33}=3.4 C/m^2$ .<sup>10</sup> The total energy of relaxed  $P2mm$  PZT vs  $c/a$  is drawn in Fig. 3, together with that of the other two structures previously discussed. This figure shows that the relaxed  $P2mm$  PZT structure has a total energy very close to that of the  $Cm$  PZT.

### F. Discussion

Experimentally, Guo *et al.* showed that the piezoelectric elongation in tetragonal PZT is along the direction associated with a monoclinic distortion,<sup>34</sup> suggesting the mechanism of polarization rotation via the monoclinic phase in PZT. This mechanism is supported by our calculations. In  $PbTiO_3$ , by contrast, although we have shown that polarization rotation does occur under applied strain, the energy difference between the tetragonal and rhombohedral structures is large, implying the need for unrealistically large applied stress or electric field. The polarization rotation we predict in PZT can occur, however, since the energy differences (see Fig. 3) are much smaller. The existence of energetically close structures in PZT 50/50 indicates that it is relatively easy to rotate the polarization from the  $[100]$  to the  $[111]$  direction in ceramic PZT. Fu<sup>35</sup> found similar energetically close states for a PZT model with Zr/Ti chemical ordering along the  $[111]$  direction. He found that the  $I4mm$  tetragonal and  $R3m$  rhombohedral structures have nearly the same total energy. Referring to Figs. 2 and 3, the ground state of our artificial chemically ordered PZT 50/50  $[001]1:1$  crystal is not near the critical region around  $c/a=1.045$ , where the largest piezoelectric coefficients are found. Our PZT 50/50 model would have to be subject to external strain to be in this critical region. Given the relatively small energy differences between the calculated structures, it is not unlikely that real disordered PZT is indeed in a condition of frustrated internal strains. Our calculations then suggest that large piezoelectric coefficients similar to those measured arise from the relatively easy rotation of the polarization between the  $[001]$  and  $[111]$  directions via locally monoclinic symmetry structures.

#### IV. CONCLUSIONS

We have reported calculations of the piezoelectric tensor coefficients in PZT 50/50, which is near the composition that defines the morphotropic phase boundary. These *ab initio* calculations yield a large piezoelectric response in PZT. This was shown to result from the rotation of the polarization in the monoclinic  $Cm$  mirror plane, and the size of the piezoelectric coefficients is commensurate with measured values in  $B$ -site disordered ceramic PZT. These calculations support the view that the large piezoelectric response of PZT close to the morphotropic phase boundary is related to the recently discovered existence of an intermediate monoclinic phase in a narrow compositional range near the morphotropic phase

boundary. Thus the presence of energetically close phases near the morphotropic phase boundary facilitates continuous atomic rearrangements leading to polarization rotation at the atomistic scale. The giant piezoelectric response found in PMN-PT and PZN-PT near the morphotropic phase boundary may have a similar origin.

#### ACKNOWLEDGMENTS

This work was supported by the Office of Naval Research (ONR) Grant No. N000149710049. We acknowledge computing support from the Center for Piezoelectrics by Design under ONR Grant No. N000140110365.

- 
- <sup>1</sup>K. Uchino, *Piezoelectric Actuators and Ultrasonic Motors* (Kluwer Academic, Boston, 1996).
- <sup>2</sup>S.-E. Park and T.E. ShROUT, J. Appl. Phys. **82**, 1804 (1997).
- <sup>3</sup>H. Fu and R. Cohen, Nature (London) **403**, 281 (2000).
- <sup>4</sup>B. Noheda, D.E. Cox, G. Shirane, J.A. Gonzalo, L.E. Cross, and S.-E. Park, Appl. Phys. Lett. **74**, 2059 (1999).
- <sup>5</sup>L. Bellaiche, A. Garcia, and D. Vanderbilt, Phys. Rev. Lett. **84**, 5427 (2000).
- <sup>6</sup>B. Noheda, D.E. Cox, G. Shirane, S.-E. Park, L. Cross, and Z. Zhong, Phys. Rev. Lett. **86**, 3891 (2001).
- <sup>7</sup>D. Vanderbilt and M.H. Cohen, Phys. Rev. B **63**, 094108 (2001).
- <sup>8</sup>G. Sági-Szabó, R.E. Cohen, and H. Krakauer, Phys. Rev. Lett. **80**, 4321 (1998), but there is an arithmetic error in their Table IV: the reported a value of  $e_{33}=3.23$  should be 3.61, which is the sum of the homogeneous and internal strain values of  $-0.98$  and  $4.59$ , respectively.
- <sup>9</sup>G. Sági-Szabó, R.E. Cohen, and H. Krakauer, Phys. Rev. B **59**, 12 771 (1999).
- <sup>10</sup>L. Bellaiche and D. Vanderbilt, Phys. Rev. Lett. **83**, 1347 (1999).
- <sup>11</sup>L. Bellaiche and D. Vanderbilt, Phys. Rev. B **61**, 7877 (2000).
- <sup>12</sup>D.A. Berlincourt, C. Cmolik, and H. Jaffe, Proc. IRE **48**, 220 (1960).
- <sup>13</sup>Z.Q. Zhuang, M.J. Haun, S.J. Jang, and L.E. Cross, in *Proceedings of the Sixth IEEE International Symposium on the Application of Ferroelectrics*, edited by V.E. Wood (IEEE, New York, 1986), p. 394.
- <sup>14</sup>M. Fornari and D.J. Singh, in *Fundamental Physics of Ferroelectrics*, edited by H. Krakauer, Ann. Isr. Phys. Soc. No. **582** (AIP, Melville, 2001), p. 23.
- <sup>15</sup>Z. Wu and H. Krakauer, in *Fundamental Physics of Ferroelectrics 2002*, edited by H. Krakauer, Ann. Isr. Phys. Soc. No. **626** (AIP, Melville, 2002), p. 9, reported some preliminary results.
- <sup>16</sup>D. Singh, *Planewaves, Pseudopotentials and the LAPW Method* (Kluwer Academic, Boston, 1994).
- <sup>17</sup>B. Noheda, D.E. Cox, G. Shirane, R. Guo, B. Jones, and L. Cross, Phys. Rev. B **63**, 014103 (2001).
- <sup>18</sup>H.J. Monkhorst and J.D. Pack, Phys. Rev. B **16**, 1748 (1977).
- <sup>19</sup>R. Yu, D. Singh, and H. Krakauer, Phys. Rev. B **41**, 6411 (1991).
- <sup>20</sup>B. Noheda, J.A. Gonzalo, L.E. Cross, R. Guo, S.-E. Park, D.E. Cox, and G. Shirane, Phys. Rev. B **61**, 8687 (2000).
- <sup>21</sup>R.D. King-Smith and D. Vanderbilt, Phys. Rev. B **47**, 1651 (1993).
- <sup>22</sup>R. Resta, Rev. Mod. Phys. **66**, 899 (1994).
- <sup>23</sup>R.M. Martin, Phys. Rev. B **4**, 1607 (1972).
- <sup>24</sup>S. de Gironcoli, S. Baroni, and R. Resta, Phys. Rev. Lett. **62**, 2853 (1989).
- <sup>25</sup>D. Vanderbilt, J. Phys. Chem. Solids **61**, 147 (2000).
- <sup>26</sup>J.F. Nye, *Physical Properties of Crystals* (Oxford University, New York, 1985).
- <sup>27</sup>M. Posternak, A. Baldereschi, H. Krakauer, and R. Resta, Phys. Rev. B **55**, 15 983 (1997).
- <sup>28</sup>W. Zhong, R. King-Smith, and D. Vanderbilt, Phys. Rev. Lett. **72**, 3618 (1994).
- <sup>29</sup>R. Resta, M. Posternak, and A. Baldereschi, Phys. Rev. Lett. **70**, 1010 (1993).
- <sup>30</sup>*Ferroelectrics: Oxides, Landolt-Bornstein Numerical Data and Functional Relationships in Science and Technology*, edited by T. Mitsui and E. Nakamura, Landolt-Börnstein, New Series, Group III, Vol. 28, Pt. a (Springer-Verlag, London, 1996).
- <sup>31</sup>L. Bellaiche, A. Garcia, and D. Vanderbilt, Phys. Rev. B **64**, 060103 (2001).
- <sup>32</sup>B. Jaffe, W. R. Cook, and H. Jaffe, *Piezoelectric Ceramics* (Academic Press, London, 1971).
- <sup>33</sup>X.H. Du, J. Zheng, U. Belegundu, and K. Uchino, Appl. Phys. Lett. **72**, 2421 (1998).
- <sup>34</sup>R. Guo, L.E. Cross, S.-E. Park, B. Noheda, D.E. Cox, and G. Shirane, Phys. Rev. Lett. **84**, 5423 (2000).
- <sup>35</sup>H. Fu, Phys. Rev. B **66**, 214114 (2002).